

# Dielectric Measurements of Semi-insulating Liquids and Solids

A.P. Washabaugh\*, A. Mamishev, Y. Du, and M. Zahn

Massachusetts Institute of Technology  
 Department of Electrical Engineering and Computer Science  
 Laboratory for Electromagnetic and Electronic Systems  
 Cambridge, MA 02139, (USA)

## Abstract

Sinusoidal steady state and transient decay measurement techniques were used to monitor the dielectric properties of electrical insulation. Impedance measurements of an air-gap capacitor, immersed in Shell Diala A transformer oil and driven with a 1 V peak sinusoidal signal (5 mHz–10 kHz), showed that the oil conductivity increased with temperature (15–70°C) and aging in air but was independent of the oil moisture content (2–30 ppm). Interfacial double layer effects were also observed.

Surface charge effects were studied in a cylindrical electrode apparatus with EHV-Weidmann Hi-Val pressboard on the inner cylinder and transformer oil filling the gap. The pressboard dielectric properties were obtained from time transient decay measurements of the open-circuit voltage after disconnecting a DC voltage source from across the cylinders. These measurements indicate that the conduction mechanism through the pressboard follows a drift dominated unipolar conduction law rather than ohmic conduction.

Further frequency sweep dielectrometry measurements using a three-wavelength interdigital electrode sensor confirm the dispersive properties of oil-impregnated pressboard. This sensor was also used to measure the time and space distributions of moisture diffusion into oil-impregnated pressboard.

## 1 Introduction

The dielectric properties of electrical insulation play an essential role in determining the integrity of power apparatus. Under normal operating conditions, the dielectric integrity can be reduced as the materials age or absorb water. The dielectric properties also determine the time constant and field distribution associated with other phenomena such as flow electrification. Consequently, it is important to have the capability of accurately measuring and monitoring the dielectric properties of the insulation. This paper describes several methods for measuring the dielectric properties of solid and liquid insulation in the time and frequency domains.

\*Now with Raychem Corporation, Menlo Park, CA.

## 2 Bulk Liquid Measurements

The liquid dielectric properties were determined by immersing an air-gap variable capacitor in the liquid and measuring the impedance over a range of frequencies. These impedances were then used to determine element values in an equivalent electrical circuit, where each element was a lumped parameter representation of the liquid dielectric properties.

The test cell impedance was determined by connecting the cell to the circuit shown in Fig. 1 and measuring the voltage gain and phase across the circuit ( $v_o/v_s$ ) as a function of frequency. The voltage source generated a sinusoidal signal having a peak amplitude of 1 V at a frequency that could be varied from 5 mHz to 10 kHz [1].

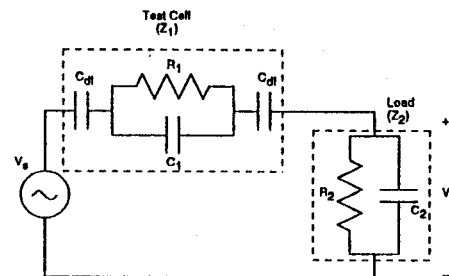


Figure 1: An electrical circuit diagram for the liquid dielectric gain and phase measurements.

The test cell impedance can be related to the measurements of the gain and the phase. With the circuit in sinusoidal steady state and the known load  $Z_2$  composed of a resistor  $R_2$  in parallel with a capacitor  $C_2$ , the impedance  $Z_1 = Z_{1r} + jZ_{1i}$  can be determined as

$$Z_{1r} = \frac{R_2 \left[ \left( \frac{1}{|G|} \cos \phi - 1 \right) - \frac{\omega R_2 C_2}{|G|} \sin \phi \right]}{1 + (\omega R_2 C_2)^2} \quad (1)$$

$$Z_{1i} = - \frac{R_2 \left[ \frac{1}{|G|} \sin \phi + \omega R_2 C_2 \left( \frac{1}{|G|} \cos \phi - 1 \right) \right]}{1 + (\omega R_2 C_2)^2} \quad (2)$$

with  $\omega$  the angular frequency,  $|G|$  the magnitude of the gain, and  $\phi$  the phase angle. For these mea-

measurements the transition frequency  $1/R_2C_2$  was chosen to be below the frequency range of the measurements by making the load the operational amplifier input impedance ( $R_2 = 1000 \text{ G}\Omega$ ) and a capacitor ( $C_2 = 750 \text{ pF}$ ).

A lumped element model for the impedance is then used to determine the bulk conductivity and permittivity of the liquid. While the simplest model for the dielectric is a resistor  $R_1$  in parallel with a capacitor  $C_1$ , this model is inadequate for describing the data. If the unknown impedance were formed by a resistor in parallel with a capacitor, a plot of the imaginary part of the impedance against the real part of the impedance would be a semi-circle. While this applies at the lower temperatures, the semi-circular shape is lost at the higher temperatures, as illustrated by the Cole-Cole plots in Fig. 2. This is consistent with capacitive elements at the electrodes and motivates the form of the test cell impedance illustrated in Fig. 1. The electrode capacitances  $C_{dl}$  result from the space-charge polarization associated with the electrical double layer while the bulk properties of the liquid are given by  $R_1$  and  $C_1$ . The lumped elements are related to the liquid dielectric properties by

$$C_1 = \frac{\epsilon A}{d - 2\lambda_D}; R_1 = \frac{d - 2\lambda_D}{\sigma A}; C_{dl} = \frac{\epsilon A}{\lambda_D} \quad (3)$$

with  $A$  the area,  $d$  the electrode spacing,  $\sigma$  the liquid conductivity,  $\epsilon$  the liquid permittivity and with  $\lambda_D$  the characteristic Debye length over which the space-charge is distributed. The geometric factor  $A/d$  is determined by measuring the capacitance of the structure in air  $C_{air}$ .

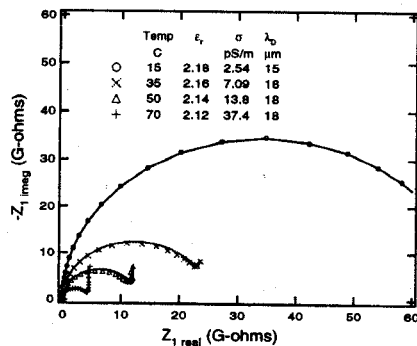


Figure 2: Representative impedance measurements for Shell Diala A transformer oil at four temperatures. The lines give the calculated impedances for the listed estimated parameters.

In this model three material properties are unknown: the permittivity, the conductivity, and the Debye length. Estimating these properties requires a minimum of two impedance measurements. With the permittivity of the fluid obtained from a high frequency measurement, a low frequency measurement (such as 10 mHz, where the double layer effects are apparent) can be used with Eq. 3 and the model test

cell impedance to give

$$\sigma = \frac{\epsilon_0}{C_{air}Z_{1r}} (1 + \omega\epsilon_r C_{air}Z_{1i}) \quad (4)$$

$$\frac{\lambda_D}{d} = -\frac{\omega\epsilon_r C_{air}}{2} \left( Z_{1i} + \frac{\omega\epsilon_r C_{air}Z_{1r}^2}{1 + \omega\epsilon_r C_{air}Z_{1i}} \right) \quad (5)$$

This approach was used to estimate the material properties and generate the lines given in Fig. 2. This relatively simple approach fits the data well.

Representative results are listed in Table 1 for two other tests. The variation in the oil permittivity with temperature provides an indication of the accuracy of the measurements; since the relative permittivity  $\epsilon_r = \epsilon/\epsilon_0$  should be constant at 2.2, the slight error is attributed to a small unmodeled parasitic capacitance. Table 1 also includes the estimated Debye lengths and the associated values for the molecular diffusivity  $D$ , calculated from  $\lambda_D = \sqrt{\epsilon D/\sigma}$ . These values show that the Debye length is roughly  $20 \mu\text{m}$  and the diffusivity increases with temperature.

Test	Temp °C	$\epsilon_r$ 10kHz	$\sigma$ (pS/m) 0.01Hz	$\lambda_D$ $\mu\text{m}$	$D$ $10^{-11} \text{ m}^2/\text{s}$
1	15	2.18	2.54	15	3.0
	35	2.16	7.09	18	12
	50	2.14	13.8	18	24
	70	2.12	37.4	18	65
2	15	2.16	1.22	9.9	0.62
	70	2.10	13.0	20	28
	15	2.16	1.25	7.6	0.38
	35	2.14	3.48	17	5.3
	50	2.12	7.03	18	12
	70	2.11	14.5	19	28

Table 1: Representative estimated properties for two oil samples.

Since many failures of electric power transformers associated with flow electrification have occurred under "dry" conditions, water has been implicated as a significant factor in the electrification process. One role that the water may play is in the creation of ionizable species in the bulk of the oil. To test if the oil moisture content affected the conductivity, an air gap capacitor, a Harley moisture sensor, and a thermocouple probe were immersed in a beaker of Shell Diala A transformer oil. The oil was mixed by a magnetic stirrer and open to atmosphere at the top. Heating tape was wrapped around the beaker and a temperature controller was used to maintain a constant temperature. The moisture content of the oil was varied by bubbling dry nitrogen gas through a porous plate diffuser immersed in the oil. After reaching a low moisture content, typically on the order of 1 ppm, the nitrogen gas was shut off and moisture from the air slowly raised the oil moisture content.

Representative conductivity measurements as the moisture content was varied is shown in Fig. 3. For these measurements, dry nitrogen was bubbled through the oil and then turned off prior to obtaining the data. The measurements show that the oil conductivity is essentially independent of the moisture

content. These results agree with those of Itahashi, et al [2] but disagree with those of Higaki, et al [3], possibly because the system studied by Higaki, et al included pressboard which may have released impurities into the oil. The apparent increase in conductivity with moisture content at 70°C is probably due to oil oxidation, rather than moisture, since the oil was exposed to air.

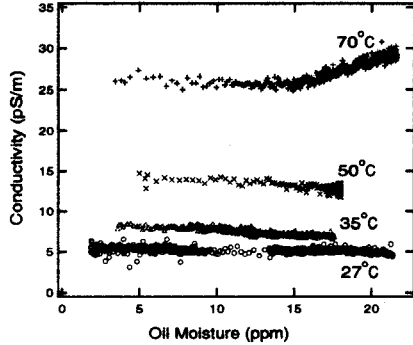


Figure 3: Electrical conductivity for Shell Diala A transformer oil as the moisture content and temperature are varied.

### 3 Time Transient Results

The dielectric properties of pressboard insulation were determined from terminal measurements made between the inner and outer cylinders of a cylindrical electrode apparatus used primarily to study flow electrification [4]. In this study, 1 mm thick EHV-Weidmann Hi-Val pressboard covered the inner cylinder and Shell Diala A transformer oil filled the remainder of the (2.5 cm) gap between the cylinders. The system was charged by applying a 22.5 V battery between the inner and outer cylinders or by rotating the inner cylinder to redistribute the charge by flow electrification. All terminal discharging measurements were performed with a stationary inner cylinder. The discharging open-circuit voltage decay was measured by an electrometer connected from the inner cylinder to the grounded outer cylinder.

A representative set of measurements of the open-circuit voltage are given in Fig. 4. The dashed lines are the result of a least squares fit to two different expressions. The “ohmic” expression is given by

$$v_{oc}(t) = Ae^{-t/\tau_{pb}} + Be^{-t/\tau_{oil}} \quad (6)$$

while the “non-ohmic” expression has the form

$$v_{oc}(t) = \frac{A}{1 + t/\tau_{pb}} + Be^{-t/\tau_{oil}} \quad (7)$$

with  $A$ ,  $B$ , and  $\tau_{pb}$  estimated parameters and  $\tau_{oil}$  the oil relaxation time, assumed to be known from oil dielectric measurements. The relatively poor fit between the “ohmic model” of (6) and the data can be attributed to the non-ohmic response of the pressboard. This is consistent with AC dielectrometry measurements showing the pressboard properties varying as a function of frequency (see Fig. 6

and [1]). The non-ohmic expression results from a unipolar migration model for charge transport that is dominated by the self-precipitation of the charged species [5].

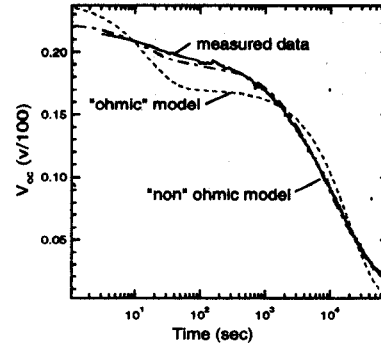


Figure 4: Representative open-circuit voltage decay measurements and fits to analytical expressions.

## 4 Interdigital Sensor

### 4.1 Description of the Sensor

Each wavelength of the three-wavelength interdigital sensor shown in Fig. 5 has electric scalar potential obeying Laplace’s equation. Neglecting variations in the  $x$  direction, the solution for each wavelength can be written as an infinite series of sinusoidal Fourier modes of fundamental spatial wavelength  $\lambda$  in the  $y$  direction that decays away in the  $z$  direction [1]:

$$\Phi(y, z) = \sum_{n=1}^{\infty} \Phi_n \text{trig}(k_n y) \text{hyp}(-k_n z), \quad (8)$$

where  $\text{trig}(k_n y)$  stands for any trigonometric function,  $\text{hyp}(-k_n z)$  stands for any hyperbolic function, and  $k_n = 2\pi n/\lambda$  is the wavenumber of each mode. For heterogeneous media, spatial profiles of dielectric properties can be determined using multiple wavelength sensors, as each wavelength has a different penetration depth into the dielectric in contact with the sensor.

For each wavelength, one set of electrodes is driven with a variable frequency AC voltage and a high impedance measurement is made of the induced voltage on the alternate set of interdigitated electrodes. The magnitude  $G$  and phase  $\phi$  of this floating voltage depend on the permittivity  $\epsilon$  and electrical conductivity  $\sigma$  of the medium adjacent to the sensor. With three different penetration depths it is possible to calculate spatial profiles of permittivity and conductivity from the gain and phase of the floating voltage as a function of frequency for each sensor wavelength [6].

### 4.2 Equilibrium Measurements

A frequency scan (5 mHz to 10 kHz) was measured in oil-impregnated pressboard in equilibrium under ambient air at 70°C. Using a parameter estimation program for homogeneous materials that relates

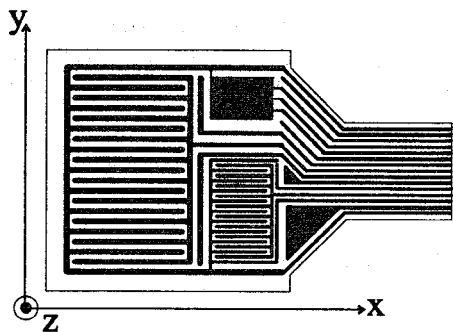


Figure 5: The three-wavelength interdigital sensor with wavelengths of 5, 2.5, and 1 mm.

measured gain and phase to complex permittivity  $\epsilon = \epsilon' - j\epsilon''$  [6], we obtain the dielectric spectrum in Fig. 6. The three wavelengths approximately give the same value indicating that the moisture distribution is essentially uniform throughout the pressboard. The relative permittivity at 60 Hz is about 4.0 which is consistent with manufacture's specifications. The difference of  $\epsilon'$  at low frequency may be due to the electrical double layer as discussed in Section 2. By linear regression, the slope of the  $\epsilon'$  curve is -0.7, indicating that it is dispersive, i.e., the conductivity changes with frequency. A constant conductivity would have a slope of  $\log \epsilon''$  versus  $\log f$  of -1 [1]. This verifies the non-ohmic property discussed in Section 3.

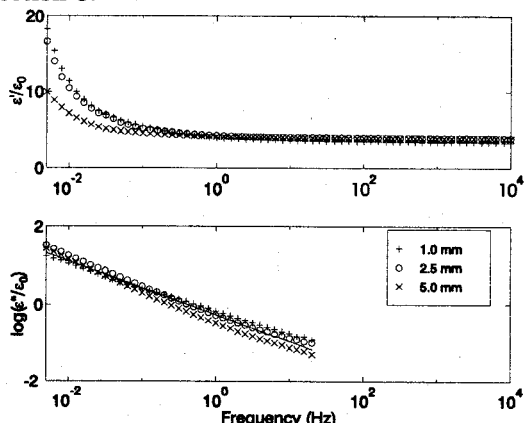


Figure 6: Dielectric spectrum for 2 mm thick oil-impregnated EHV-Weidmann Hi-Val pressboard at ambient air in equilibrium at 70°C.

### 4.3 Non-equilibrium Measurements

One piece of 1.0 mm thick EHV-Weidmann Hi-Val pressboard was oil-impregnated in the test chamber under vacuum with dry Shell Diala A transformer oil at 70°C. At time zero in Fig. 7, wet oil with about 290 PPM moisture content was introduced into the chamber. The moisture in the wet oil started to diffuse into the dry pressboard and the diffusion process was measured by the three-wavelength sensor as shown in Fig. 7. The response of each wavelength starts to change when the moisture diffuses to the region within each penetration depth. With

response delays of 0 hours, 10 hours, and 30 hours for the 5 mm, 2.5 mm, and 1 mm wavelengths respectively, the diffusion coefficient is estimated to be about  $6.0 \times 10^{-12} \text{ m}^2/\text{s}$ , which agrees well with the literature value [7].

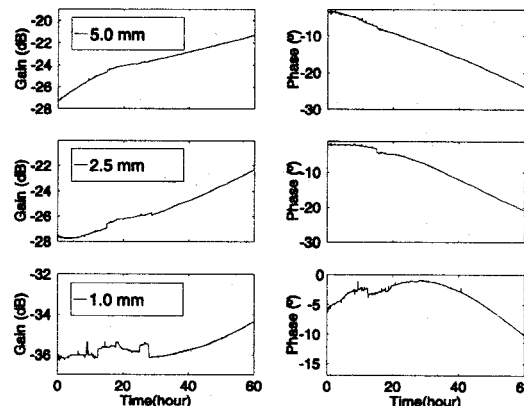


Figure 7: Gain and phase measurements of moisture diffusion process of 1 mm thick EHV-Weidmann Hi-Val oil-impregnated pressboard at 70°C and  $f=1$  Hz.

## 5 Acknowledgements

This work was supported by EPRI as Research Project 3334-1 under Mr. Stan Lindgren and a Demonstration of Energy-Efficient Developments Scholarship from American Public Power Association.

## References

- [1] Y. Sheiretov and M. Zahn, "Dielectrometry Measurements of Moisture Dynamics in Oil-Impregnated Pressboard," *IEEE Trans. Diel. and Electr. Ins.*, Vol. 2, No. 3, pp. 329-351, 1995.
- [2] S. Itahashi, H. Mitsui, T. Sato, and M. Sone, "State of Water in Hydrocarbon Liquids and its Effect on Conductivity," *IEEE Trans. Diel. and Electr. Ins.*, Vol. 2, No. 6, pp. 1117-1122, 1995.
- [3] M. Higaki, Y. Tsutsumi, H. Ohtani, and H. Tsukioka, "Consideration of the Measurement of Static Charges in Insulating Oil and the Influence of Oil Conductivity on the Charges," *Elect. Eng. in Japan*, Vol. 104, No. 5, pp. 9-17, 1984.
- [4] A.J. Morin II, M. Zahn, and J.R. Melcher, "Fluid Electrification Measurements of Transformer Pressboard/Oil Insulation in a Couette Charger," *IEEE Trans. Electr. Ins.*, Vol. 26, No. 5, pp. 870-901, 1991.
- [5] M. Zahn, "Drift-dominated Conduction Within an Ohmic Medium," *J. Appl. Phys.*, Vol. 47, No. 7, pp. 3122-3126, Jul 1976.
- [6] P. A. von Guggenberg, "Application of Interdigital Dielectrometry to Moisture and Double Layer Measurements in Transformer Insulation," Ph.D. Thesis, EECS Department, MIT, 1993.
- [7] S.D. Foss, "Power Transformer Drying Model," Report prepared for General Electric Company, Large Transformer Operation, Pittsfield, MA, and Consolidated Edison Corporation, New York, NY, by Dynamic Systems, Pittsfield, MA, 1987.